

# THE FABRICATION AND COLD TEST OF A HIGH BRIGHTNESS X-BAND RF GUN

C.H. Ho, W.K. Lau, T.T. Yang, J.Y. Hwang, S.Y. Hsu, Y.C. Liu

Synchrotron Radiation Research Center, Hsinchu, Taiwan

G.P. Le Sage, F.V. Hartemann, and N.C. Luhmann, Jr.

University of California at Davis, Department of Applied Science, Davis, CA, USA

## ABSTRACT

A recently proposed [1] high brightness, high repetition rate, multibunch photoinjector project has reached the prototype testing stage. The accelerator structure consists of a 1-1/2 cell, side wall coupled, X-Band (8.548 GHz) standing wave cavity, driven by a 20 MW SLAC Klystron, and a GHz repetition rate (burst mode) rf modelocked AlGaAs laser diode oscillator and CPA Ti:Al<sub>2</sub>O<sub>3</sub> multipass amplifier. The photocathode gun will be used to accelerate a train of one hundred 1 nC electron bunches to an energy in the range of 5 MeV. A joint collaboration between the UC Davis Department of Applied Science (DAS), and the Synchrotron Radiation Research Center (SRRC) has been established to expedite the construction and characterization of the accelerator structure. A prototype copper cavity has been fabricated and characterized. The results of the low power rf measurements are presented.

## 1 INTRODUCTION

The requirements of high brightness and high intensity for relativistic electron beams for Free Electron Laser (FEL) and laser scattering and acceleration experiments have made the photoinjector an attractive source. Since the invention of the photoinjector in the mid eighties, variations of the concept have been used for FEL experiments, high luminosity colliders, sources of high charge pulses for wakefield accelerators, and low emittance beams for general high energy physics research.

Recently, a multibunch photoinjector project was proposed at 8.548 GHz, which produces a compact structure with higher accelerating gradients, and thus lower emittance characteristics than the existing rf guns whose frequencies typically range from 100 MHz to 3 GHz. The X-Band frequency is also low enough to avoid limiting tolerance requirements, as well as deleterious wakefield effects associated with RF structures designed for very high frequencies.

Another distinguishing feature of this project is the high

repetition rate of the synchronized laser system. The laser and RF systems are driven by a single, highly stable crystal oscillator. The laser system is based on an rf modelocked AlGaAs diode oscillator, modelocked at the fourth subharmonic of the Klystron rf frequency, which has a measured jitter of 400 fs rms over a 100 second measurement period. A train of one hundred pulses are switched out of this oscillator, and amplified by an 8-pass, 10<sup>-6</sup> gain, chirped pulse Ti:Al<sub>2</sub>O<sub>3</sub> amplifier. The pulse train is then frequency quadrupled to 208 nm using a pair of BBO crystals. While the total effective charge in each macropulse is increased by a factor of one hundred, the low emittance characteristics associated with the charge of the micropulse (0.1 - 1 nC) is maintained. An alternate Ti:Al<sub>2</sub>O<sub>3</sub> oscillator is also available in the laser system which produces 100 fs IR pulses with a repetition rate of 134 MHz. The output of this oscillator will be passed through a series of beam splitters and optical delay lines to increase the repetition rate by a factor of 4, corresponding to the 16th subharmonic of the rf drive. A photodiode is used to produce an rf signal which can be frequency multiplied and amplified to drive the rf system in an alternate configuration to the diode oscillator system.

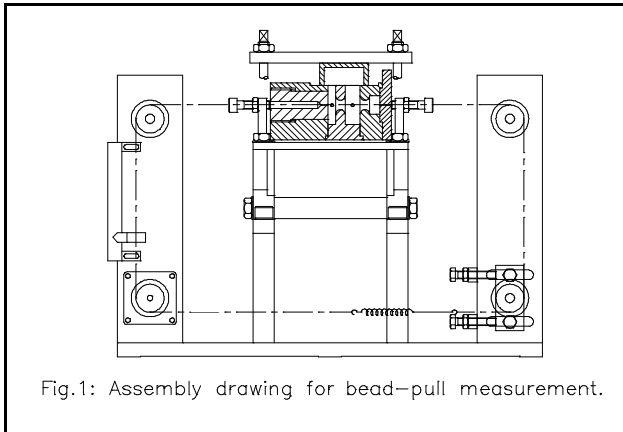
A collaborative research effort for the rapid development of the X-Band photoinjector system has been formed between UC Davis DAS, and SRRC. A prototype X-Band structure has been fabricated by SRRC, and continues to be characterized by UC Davis DAS at the Lawrence Livermore National Laboratory (LLNL) site. Both the design and fabrication procedures have included separate verification from both groups. The high power, ultra-high vacuum, brazed structure will also be constructed at SRRC. The gun will be installed and fully characterized at LLNL by the UC Davis DAS personnel.

## 2 PROTOTYPE FABRICATION

The initial prototype RF cavity is a scaled version of the S-Band Brookhaven gun. Extensive simulation runs using the codes SUPERFISH and PARMELA predict an energy of 4.3 MeV with a peak gradient of 150 MV/m, corresponding to a drive power of 9 MW. With a microbunch charge of 0.1

nC, the predicted transverse, rms, invariant emittance is less than  $1 \pi$  mm-mrad. The energy spread for this case is 0.31 % at the gun exit. A prototype copper cavity was fabricated in a CNC machine shop near the SRRC facility. The measured accuracy of the machining tolerance is  $\pm 0.05$  mm. A supporting structure made of Aluminum was also built for the purposes of bead pull cavity perturbation measurements.

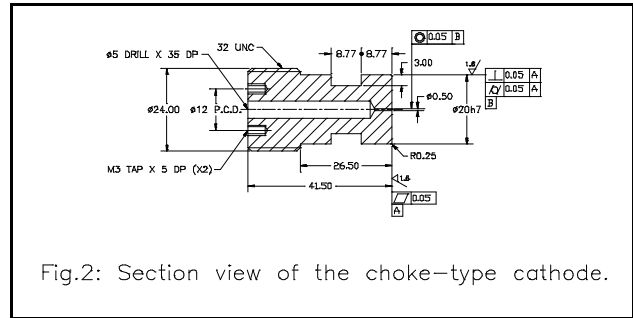
The central frame, which is used to press together the cavity components, is detachable from the supporting stand, and can be used to test a variety of cavity structures. The experimental arrangement for the bead pull measurements is shown in Fig. 1. A machinable ceramic (Aluminum Oxide) bead with a 1.2 mm diameter was used as an axial cavity perturbation. The bead was drilled using an Nd:Yag laser, and a nylon string with diameter 0.05 mm was used to pull the bead down the axis of the cavity. A 0.69 mm length, 0.49 mm diameter metal cylinder, made from a section of a hypodermic needle has also been used to check the convergence of the bead pull data.



A steel alignment pin was placed in a groove along the outer edge of the cavity body to avoid rotation of the separate sections of the cavity. For the purposes of the cold test, the waveguide lateral position was not fixed, but free to be moved and optimized. The waveguide can be moved over a distance  $\pm 7$  mm.

The large diameter of the cathode (20 mm) has the purpose of avoiding the well known problems of rf breakdown and field emission leading to dark current near the gap between the cathode plug and cavity wall by moving the gap to a low field region. A 32 UNC threaded cathode plug was originally used to make the fine adjustments of the cathode position. A BAL SEAL coil spring is placed in a groove near the cathode surface to provide a short path for the wall currents which leak into the gap region. The contact of the clean, tight tolerance copper surfaces of the cathode plugs was found to cause galling problems initially with the coil spring arrangement. A choke type cathode was built to alleviate this problem, as shown in Fig. 2. The choke type plunger is based on the principle of a quarter-wave transformer. This type of cathode seems to produce similar results to that of the coil

spring arrangement. The galling problem eventually persisted, even with the choke type cathode plug. By using a micrometer and avoiding the twisting motion of the plug inside the cavity, the problem of galling seems to have been eliminated to the point where we may reconsider the coil spring arrangement, or even a combination of the two techniques.



Coupling to the accelerator structure is accomplished through two apertures in the broad wall of a  $TE_{10}$  waveguide, and side wall apertures in the full and half cell cavities. The coupling occurs through the  $\phi$  component of the  $TM_{010}$  mode magnetic fields in the cavities, and the axial magnetic field component in the waveguide. This waveguide axial field is phased 180 degrees apart on either side of the broad wall center line, and leads to the dominant excitation of the  $\pi$ -mode in the cavities. The wall currents are also useful for visualizing the coupling between the fundamental modes in the waveguide and cavities, and also demonstrates the  $\pi$ -mode dominance. The lateral position of the waveguide strongly effects the relative coupling of the cells since the magnetic field reaches a null in the center of the waveguide. When the half cell aperture is near the edge of the broad wall of the waveguide, the resonance peak becomes significantly deeper than that of the full cell, when these resonances are detuned. The case where the full cell aperture is near the outer waveguide edge produces an even more pronounced effect, since the aperture in the full cell is longer than that of the half cell. Unfortunately, the situation is even more complicated when the resonance peaks are close together, since a balanced field can be achieved even when the separate resonances initially have greatly disparate amplitudes. This is due in part to coupling through the aperture between the cells.

The sizes of the coupling holes were optimized empirically, in small iterative steps, until critical coupling was achieved. The coupling is accomplished using a lateral slot with rounded ends, and started with dimensions  $18 \text{ mm} \times 2 \text{ mm}$ . Each cavity is also equipped with a field tuner and monitor. The tuners are basically rounded copper plungers which radially penetrate the outer wall of the cavity. The field monitors consist of recessed loops which couple to the  $\phi$  component of the  $TM_{010}$  mode magnetic field. The cross sectional view of the tuner and monitor assemblies are shown in Fig. 3.

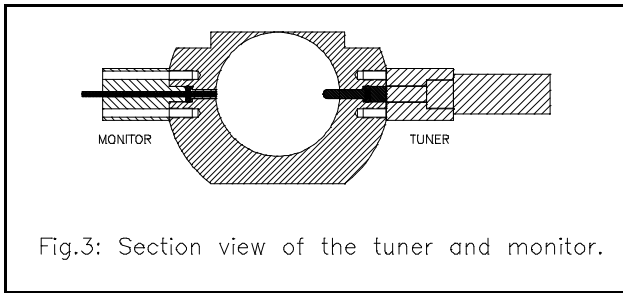


Fig.3: Section view of the tuner and monitor.

### 3 PRELIMINARY COLD TEST RESULTS

The cavity optimization procedure is as follows. A sliding short plate at one end of the feed waveguide is adjusted to a distance of  $N \times L_g + 3/4 L_g$  from the center of the coupling hole. The standing wave peak in the guide is thus maximized over the coupling apertures. The frequencies of the half cell and full cell are initially detuned so that their resonances do not overlap. The waveguide lateral position is then adjusted until the magnitude of the reflection coefficient for the half cell and full cell are roughly equal. This assures that rf power is coupled into the separate cells with similar amplitude. The field tuners are then used to merge the resonances of the half cell and full cell. A bead pull measurement is performed to check the balance between the field amplitudes in the half cell and full cell. The phase from each field monitor is also

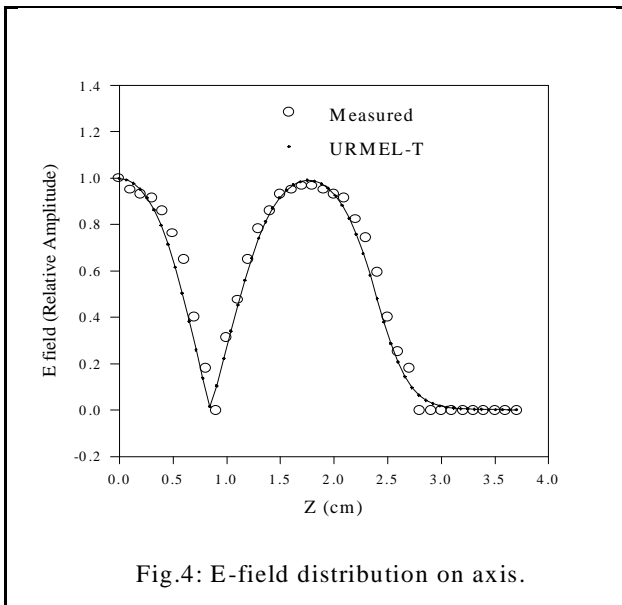


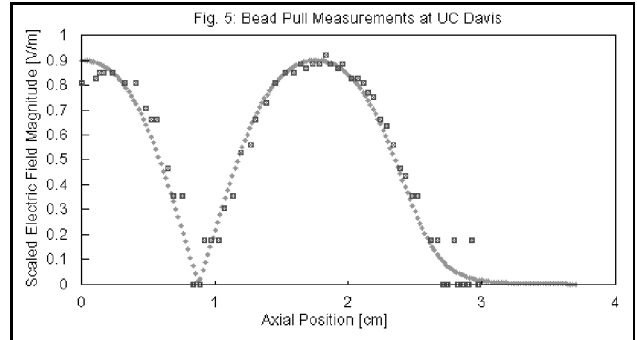
Fig.4: E-field distribution on axis.

measured to look for 180 degrees phase difference, corresponding to the  $\pi$ -mode. The monitors form a second port for the network analyzer in this case. This procedure is iterated with small changes to the size of the coupling holes.

The effect of cathode tuning is drastically larger than that

of the field tuners, obviously due to its larger diameter. The cathode plug will be tightly locked in position very nearly flush to the rear cavity wall for high power operation.

An example bead pull measurement is shown in Fig. 4 for a roughly balanced field case. We also show the consistency of the measured data with an URMEL-T calculation of the simulated field profile. A similar measurement performed at UC DAS is shown in Fig. 5, and compared to a SUPERFISH simulation of the cavity field profile.



### 4 SUMMARY

A prototype X-Band rf accelerator cavity has been fabricated at SRRC, and continues to be characterized and optimized at UC Davis DAS. Many unexpected, and very important developments have been revealed through experimentation with this test apparatus. A few of the cavity parameters continue to be optimized using this test structure. The high power OFE copper cavity will shortly be produced once these final few parameters are fully optimized.

### 5 ACKNOWLEDGEMENTS

We would like to thank Dr. G. Westenskow (LLNL) and Dr. Y.J. Chen (LLNL) for many useful discussions and suggestions. This work is supported in part by the National Science Council (Taiwan), as well as by MURI (USA) under contract F49620-95-1-0253, by ATRI (USA) under contract F30602-94-2-0001, and by DoE (USA) under contract DE-FG03-95ER54295.

### REFERENCE

- [1] G.P. Le Sage, et al., "2.142 GHz Repetition Rate High Brightness X-Band Photoinjector", in Proc. 1995 IEEE Particle Accelerator Conf. (Dallas, Texas, USA).